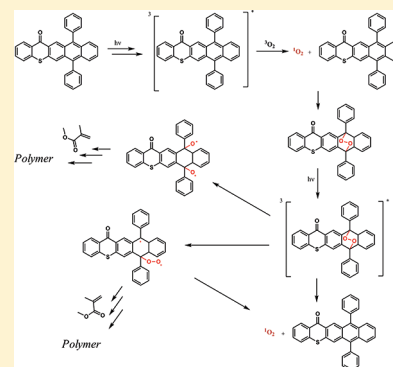


Thioxanthone–Diphenyl Anthracene: Visible Light Photoinitiator

Demet Karaca Balta, Gokhan Temel, Gokce Goksu, Nuket Ocal, and Nergis Arsu*

Department of Chemistry, Yildiz Technical University, Davutpasa Campus, Istanbul 34210, Turkey

ABSTRACT: 7,12-Diphenyl-14*H*-naphto[2,3-*b*]thioxanthen-14-one (TX-DPA) was synthesized and characterized as a potential visible light photoinitiator for radical polymerization. TX-DPA has an excellent absorption character in the visible region and the photophysical properties of TX-DPA were investigated by fluorescence and laser flash photolysis studies and the photopolymerization of methyl methacrylate in air atmosphere helped to understand the initiation mechanism of TX-DPA. Moreover, it is possible that the production of singlet oxygen from the quenching of $^3\text{TX-DPA}$ by molecular oxygen resulted in the reaction of singlet oxygen with TX-DPA to form an endoperoxide: decomposition of endoperoxide leads to initiating radicals.

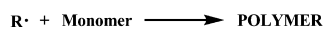
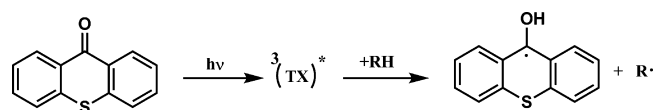


INTRODUCTION

In recent years, many attempts have been made to synthesize photoinitiators that operate in the visible region of the spectrum. The reason for this is that visible light is cheap, safe and possesses high penetration ability in the presence of UV absorbing monomers, pigments and substrates.^{1–7}

Thioxanthone (TX) and its derivatives are some of the most widely used type II photoinitiators in various UV curing applications because of their excellent light absorption characteristics.⁸ In most cases, the photoinitiating free radicals are generated by hydrogen abstraction of triplet excited states of TX from hydrogen donors such as amines or thiols (see Scheme 1).^{9–11}

Scheme 1. Photoinitiated Free Radical Polymerization Using TX as Photoinitiator



However, low molecular-weight amines, particularly when used at high concentrations, have several intrinsic disadvantages such as odor, toxicity¹² and migration in UV-curing technology and cause a decrease in the pendulum hardness of the cured film.¹³ One way to overcome these problems is to chemically incorporate the hydrogen donating sites into TX chromophores.^{14–16}

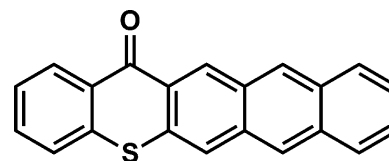
Amine,^{17–20} alkyl amino,^{21,22} acid,^{23–27} or thiol²⁸ linked photoinitiators are seen in the literature and they may find various applications in the Radiation Curing Industry because of the great advantages of their one-component nature. Because

of the one-component structure of the photoinitiator, it can serve as both a triplet photosensitizer and as a hydrogen donor during photopolymerization. Thus, these photoinitiators do not require an additional co-initiator.

An alternative approach concerns the attachment of both chromophoric and hydrogen donating groups into polymer chains.^{29–35} This way the odor and toxicity problems perceived with the conventional photoinitiators and amine hydrogen donors have been overcome.

We have also developed a novel thioxanthone based photoinitiator possessing an anthracene group, thioxanthone–anthracene³⁶ (TX-A, Chart 1), which exhibits completely different photochemical properties compared to conventional TX type photoinitiators.

Chart 1. Structure of TX-A



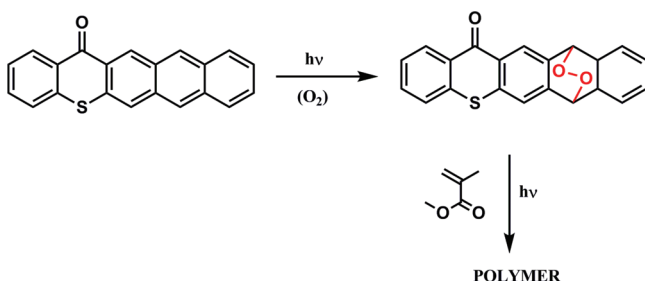
In contrast to TX type photoinitiators, TX-A is an efficient photoinitiator for free radical polymerization of both acrylic and styrenic type monomers in the presence of oxygen without an additional hydrogen donor.^{36–38} Moreover, for other TX type photoinitiators oxygen inhibits the polymerization because of the quenching of the excited triplet TX with oxygen. In the case of TX-A, molecular oxygen is essential for the initiation process. The initiation mechanism involves the formation of singlet oxygen by energy transfer from triplet TX-A³⁹ (Scheme 2).

Received: September 26, 2011

Revised: November 29, 2011

Published: December 16, 2011

Scheme 2. Photoinitiation Mechanism of TX-A in the Presence of Oxygen



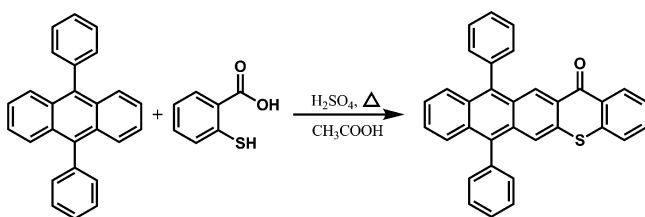
There is another possible application of using an oil soluble initiator in water; complexation of TX-A with β -CD was achieved and photopolymerization of acrylamide with TX-A/ β -CD was performed.⁴⁰

Our aim is to synthesize new photoinitiators which have absorption in the visible region and operate in oxygen atmosphere. We achieved the synthesis of 7,12-diphenyl-14*H*-naphtho[2,3-*b*]thioxanthen-14-one (TX-DPA). ¹H NMR, ¹H–¹H COSY, elemental analysis, and GC–MS were used for the characterization of TX-DPA. Photophysical properties were determined by the use of UV–vis, fluorescence and laser flash photolysis, and photoinitiated polymerization of methyl methacrylate was performed with TX-DPA by using a xenon lamp as the irradiation source.

RESULTS AND DISCUSSION

Synthesis and Characterization. The synthesis of TX-DPA was achieved by using a similar method to that which was described in our previous publication (see Experimental Section, Chart 2).³⁶ Since there are more than one ring closure

Chart 2. Synthesis of TX-DPA

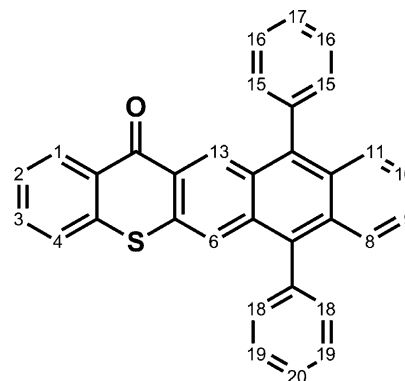


possibilities, due to the aromatic groups on the DPA (see Experimental Section, Chart 3), the COSY NMR method was employed to define the structure of the product in addition to using ¹H NMR spectroscopy.

¹H–¹H COSY was employed to confirm the structure of the compound. Figure 1 shows the ¹H–¹H COSY spectrum, the peak at 8.03 ppm as doublet is coupled with the H₁₅ proton of the phenyl group as expected, while the peak at 7.62 ppm as doublet is coupled with the proton H₁₈. The H₄ proton is determined by ¹H–¹H COSY as doublet and is clearly coupled with H₃.

Absorption and Fluorescence. TX-DPA has excellent absorption properties in the visible region of the electromagnetic spectrum and the absorption characteristics of TX-DPA were found to be very similar to the parent compounds, both thioxanthone and 9, 10-diphenylanthracene. The molar absorptivities of TX-DPA where the wavelength values were 383 and 450 nm were calculated as 10633 and 4347

Chart 3



L.mol^{−1}.cm^{−1}, respectively. These high molar absorptivity values would be beneficial for a photoinitiator in the visible region (Figure 2).

A photodecomposition study of TX-DPA was performed in CHCl₃ and this solution was exposed to UV light at certain periods of time and the photodecomposition of TX-DPA was followed by detecting UV-spectral changes (Figure 2).

At the end of the irradiation (270 s) while the typical absorption bands of the diphenylanthracene moiety from DPA completely disappeared, the weak absorption of the TX group at 380 nm was still detectable.

Fluorescence measurements were conducted in order to clarify the mechanistic details. As can be seen from Figure 3, the excitation spectrum of TX-DPA is very similar to its absorption spectrum.

The emission spectrum represents the characteristics of the TX moiety rather than DPA. The intersection of the emission and excitation spectra at 464 nm, allowed us to calculate the singlet excited state energy of TX-DPA, as ca. 257.8 kJ/mol.

The fluorescence quantum yield, ϕ_f , was estimated to be 0.45 by using 9,10-diphenylanthracene as the standard. ($\phi_f = 0.95$).^{41,42} From the calculations, the fluorescence quantum yields ($\phi_{(TX-DPA)} = 0.45$) of anthracene chromophore were more dominant than the TX [$\phi_{(TX)} = 0.07$]. This high fluorescence quantum yield reduced the triplet yield, the state from which initiating radicals are generated.

Fluorescence quenching studies of TX-DPA were performed by adding MDEA at different concentrations and the changes in the fluorescence emissions were recorded for the TX-DPA/ethanol solution. The Stern–Volmer representation (i.e., I_0/I vs $[Q]$) is shown in Figure 4. It can be observed that the least-squares fit of the experimental results produces a straight line with reasonable point scattering. The linearity of the corresponding plot was always excellent ($R^2 > 0.90$), and no deviation was detected at high quencher concentrations. The Stern–Volmer quenching constant, K_{sv} , obtained from the slope is 0.86 M^{−1}.

Laser Flash Photolysis. To investigate the properties of the triplet state and its reactivities, laser flash photolysis experiments were performed. Figure 5 shows the transient absorption spectra of TX-DPA directly after irradiation with laser pulses at 355 nm. Three transient absorption maxima were observed at 400, 490, and 590 nm (see Figure 5a) which decayed in a first-order kinetic with a lifetime of 2.6 μ s (Figure 5b). The peak at 590 nm was assigned to the triplet–triplet absorption of TX-DPA based on similarities with the triplet–triplet spectra of TX⁴³ and TX derivatives.²⁸ Recently we

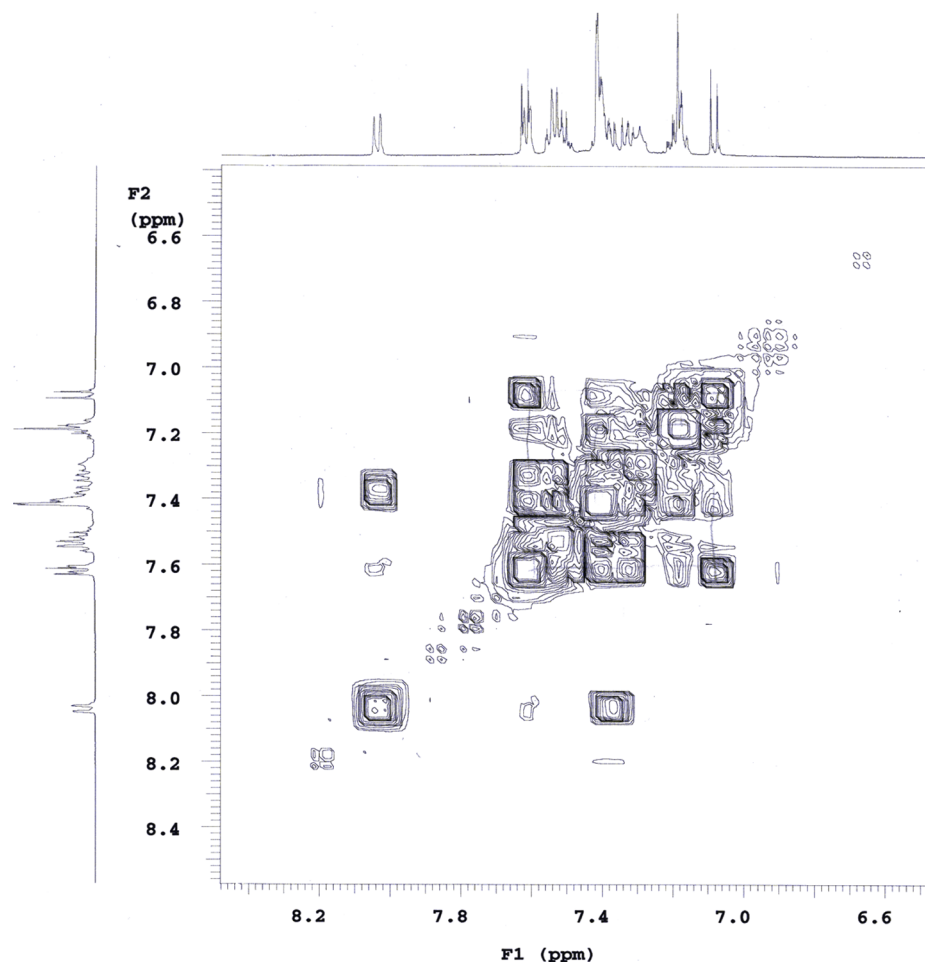


Figure 1. ^1H – ^1H COSY spectrum of TX-DPA in CDCl_3 .

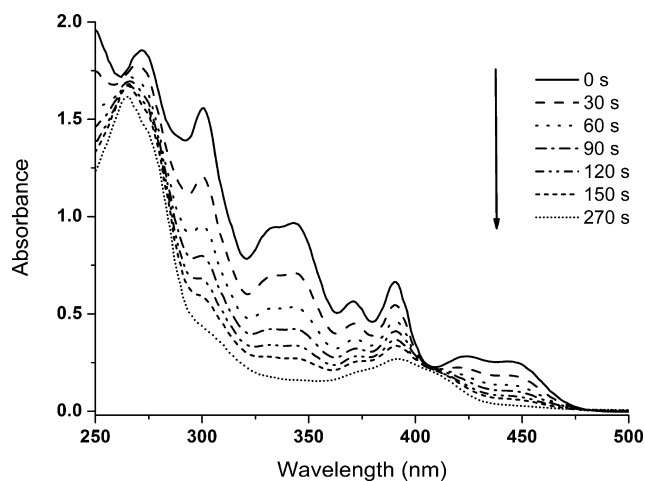


Figure 2. Photobleaching of TX-DPA [4.10×10^{-5} M] in CHCl_3 during 0–270 s in air atmosphere with polychromatic light (unfiltered light from a medium pressure mercury lamp).

submitted LFP studies of TX-A, and the triplet lifetime of TX-A was calculated as $28 \mu\text{s}$.³⁹

Notably, all transients were quenched by oxygen and were tentatively assigned to the triplet state. Quenching experiment of transients with MDEA were also achieved and the rate constant was found as $\sim 2.72 \times 10^9 \text{ M}^{-1} \text{ s}^{-1}$ (see Figure 6).

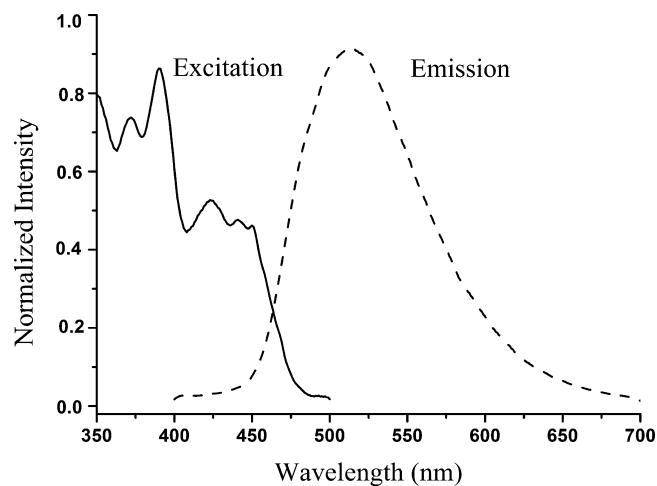


Figure 3. Fluorescence excitation (—) and emission (--) spectra of TX-DPA in ethanol; $\lambda_{\text{exc}} = 390 \text{ nm}$.

From the previous studies^{36,39} related with anthracene attached thioxanthone (TX-A), polymerization experiments in the presence and absence of oxygen clearly confirmed the crucial role of oxygen for successful polymerization as the efficient initiation of TX-A can be attributed to the formation of endoperoxide by the reaction of TX-A with singlet oxygen.

Photopolymerization. A similar way was followed to determine the initiation mechanism of TX-DPA, and polymer-

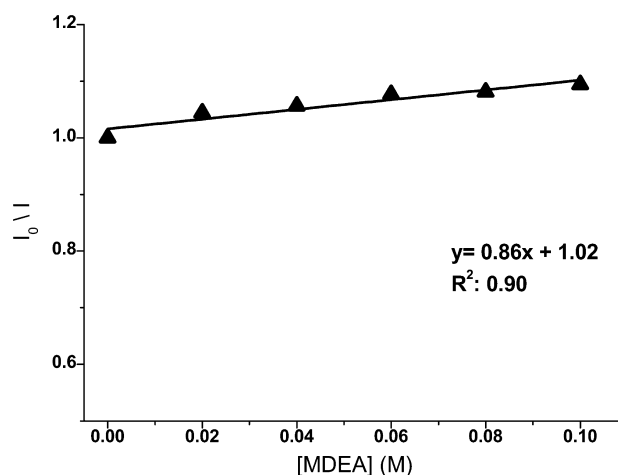


Figure 4. Stern–Volmer plot of the quenching of TX-DPA [1.0×10^{-5} mol L $^{-1}$] by MDEA in ethanol ($\lambda_{\text{exc}} = 390$ nm). I_0 = fluorescence intensity of TX-DPA, I = fluorescence intensity in the presence of MDEA.

ization experiments of methyl methacrylate with TX-DPA in DMF in the presence and absence of oxygen atmosphere were performed. Additionally, a tertiary alkyl amine namely *N*-methyldiethanolamine (MDEA) was also added to the same formulation to see the inhibition effect of oxygen beside the synergistic effect of the amine. A xenon lamp source was used as the irradiation source, since TX-DPA has excellent absorption in the visible region.

At the very low initiator concentration level (5×10^{-5} M), polymerization was not observed in air atmosphere, but when MDEA was added to this formulation in air atmosphere, the conversion percentage was found to be 3.50. When the initiator concentration increased to 1×10^{-4} M, some polymer formation was observed but the conversion percentage was still low compared to the formulation containing MDEA. By further increasing the initiator concentration to 5×10^{-4} M, the beneficial effect of oxygen for the formation of endoperoxide appeared and the conversion percentage was 5.3 in air atmosphere, 3.8 in the presence of MDEA, and 2.9 in nitrogen atmosphere. When the obtained results in the presence of amine and nitrogen atmosphere were compared, the beneficial

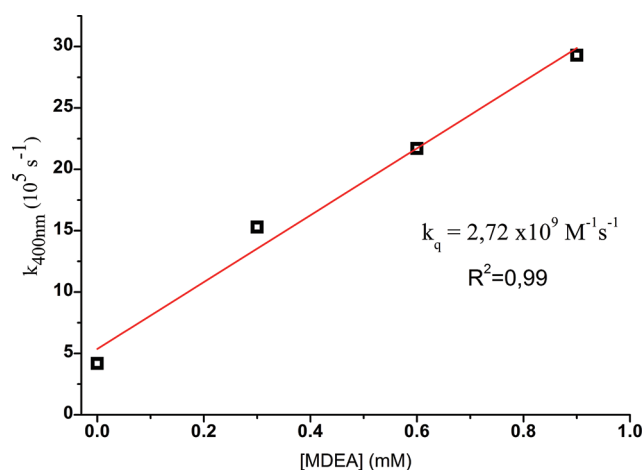


Figure 6. Reaction of MDEA with triplet TX-DPA in acetonitrile solutions 23 °C. Dependence of the pseudo-first-order rate constant of the decay of the optical absorption at 400 nm on the concentration of MDEA after laser excitation (355 nm).

effect of the amine appears to be due to the formation of α -aminoalkyl radicals (see Table 1).

Table 1. Photoinitiated Polymerization of Methyl Methacrylate [4.68 mol L $^{-1}$] in DMF with TX-DPA in the Absence and Presence of MDEA in/under a Xenon Lamp System

[TX-DPA] (mol L $^{-1}$)	[MDEA] (mol L $^{-1}$)	% convn ^a	$M_n \times 10^{-4}$ (g mol $^{-1}$)	M_w/M_n
5×10^{-5}	-	0.0	-	-
5×10^{-5}	5×10^{-2}	3.5	2.51	1.39
1×10^{-4}	-	0.7	3.50	1.40
1×10^{-4}	5×10^{-2}	4.5	2.30	1.32
5×10^{-4}	-	5.3	4.33	2.09
5×10^{-4}	5×10^{-2}	3.8	2.04	1.25
5×10^{-4}	-	2.9	3.22	1.44
1×10^{-3}	5×10^{-2}	1.2	2.39	1.24
1×10^{-3}	-	1.0	3.65	1.48

^a $t_{\text{irr}} = 60$ min. ^bUnder nitrogen atmosphere $I_{0(\text{UV-A})} = 175$ W·m $^{-2}$

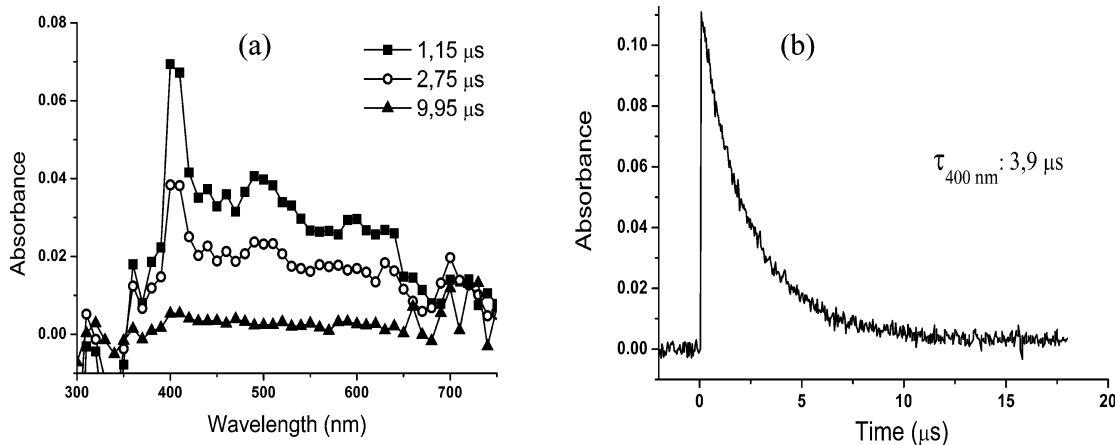


Figure 5. (a) Transient optical absorption spectrum recorded 1.15 μ s, 2.27 and 1.4 μ s following laser excitation (355 nm, 5 ns) of TX-DPA [2.4×10^{-5} M] in argon saturated acetonitrile solution at 23 °C; (b) Kinetic traces of the transient optical absorption spectrum at 400 nm recorded 1.15, 2.27, and 1.4 μ s following laser excitation (355 nm; 5 ns) of TX-DPA in argon-saturated acetonitrile solution at 23 °C.

For comparison, photopolymerization experiments using either TX or DPA themselves or their combinations in the presence and absence of the hydrogen donor MDEA were performed (Tables 2 and 3).

Table 2. Photoinitiated Polymerization of Methyl Methacrylate [4.68 mol L^{-1}] in DMF with DPA in the Absence and Presence of MDEA in/under a Xenon Lamp System

[DPA] (mol L^{-1})	[MDEA] (mol L^{-1})	% convn ^a
5×10^{-5}	-	0.0
5×10^{-5}	5×10^{-2}	3.8
1×10^{-4}	-	0.0
1×10^{-4}	5×10^{-2}	4.6
5×10^{-4}	-	0.3
5×10^{-4}	5×10^{-2}	6.7
1×10^{-3}	-	0.6
1×10^{-3}	5×10^{-2}	7.9

^a $t_{\text{irr}} = 60 \text{ min.}$

Table 3. Photoinitiated Polymerization of Methyl Methacrylate [4.68 mol L^{-1}] in DMF in the Presence of 9,10-Diphenylanthracene (DPA) and Thioxanthone (TX) in/under a Xenon Lamp System

[DPA] (mol L^{-1})	[TX] (mol L^{-1})	[MDEA] (mol L^{-1})	% convn ^a
5×10^{-4}	5×10^{-4}	-	0.6
5×10^{-4}	5×10^{-4}	5×10^{-2}	2.3

^a $t_{\text{irr}} = 60 \text{ min.}$

Anthracene derivatives are known to form instable endoperoxides upon irradiation.⁴⁴ The singlet oxygen ($^1\text{O}_2$) addition rate constant was reported in the literature^{45,46} as $5.4 \times 10^5 \text{ M}^{-1} \text{ s}^{-1}$ for anthracene and $3.0 \times 10^6 \text{ M}^{-1} \text{ s}^{-1}$ for diphenylanthracene. The singlet oxygen rate constants and stabilities of the endoperoxides increase as more electron-pushing substituents are added to the anthracene ring. The bimolecular quenching rate constant of singlet oxygen by TX-A was found to be similar to the reported value for anthracene ($k_{1\text{O}_2} = 5.4 \times 10^5 \text{ M}^{-1} \text{ s}^{-1}$).⁴⁵ These endoperoxides decompose (thermally and photochemically) through radical intermediates,^{47–49} which could initiate the polymerization of the monomers. The endoperoxide of diphenylanthracene-TX is probably formed very easily due to the stability of TX-DPA, and possibly the formation of endoperoxide is not occurring efficiently in room temperature to produce initiating alkoxy and/or peroxy radicals. This could be an explanation of the low polymer yield in the presence of TX-DPA when comparing the results obtained with TX-A as the initiator.³⁶

In air atmosphere, the initiating ability of DPA for the MMA polymerization in the presence and absence of TX was seen as proof of the formation of endoperoxide.

For the characterization of the polymer, UV spectroscopy was used. In Figure 7, the absorption spectra of TX-DPA and the poly(methyl methacrylate) obtained from the irradiation with xenon lamp in the absence of MDEA are shown. The UV absorption spectra of purified polymer produced from initiation with a high initiator concentration ($5 \times 10^{-4} \text{ M}$) showed absorbance at 300 nm, which indicates TX chromophores bound slightly to polymers.

A feasible mechanism for the initiation process involves the formation of an endoperoxide by the reaction of TX-DPA with

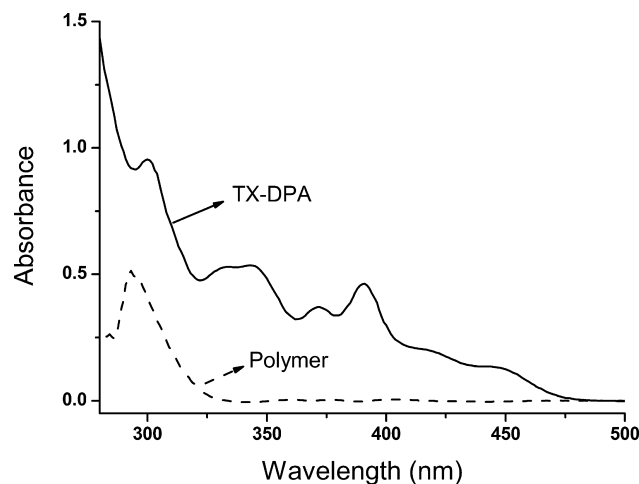


Figure 7. Absorption spectra of TX-DPA (—) and poly(methyl methacrylate) (---) obtained ([PI]: $5 \times 10^{-4} \text{ M}$) in THF.

singlet oxygen formed from the triplet excited state in the presence of oxygen as illustrated in Scheme 3. The excitation of this intermediate eventually leads to the formation of peroxy and/or alkoxy radicals capable of initiating free radical polymerization of MMA.

In the presence of MDEA, the possibility of the formation of endoperoxide is getting lower since oxygen in the medium is scavenged by MDEA. Therefore, the TX part plays a more dominant role and so a typical type II initiation mechanism appears (Scheme 4).

CONCLUSION

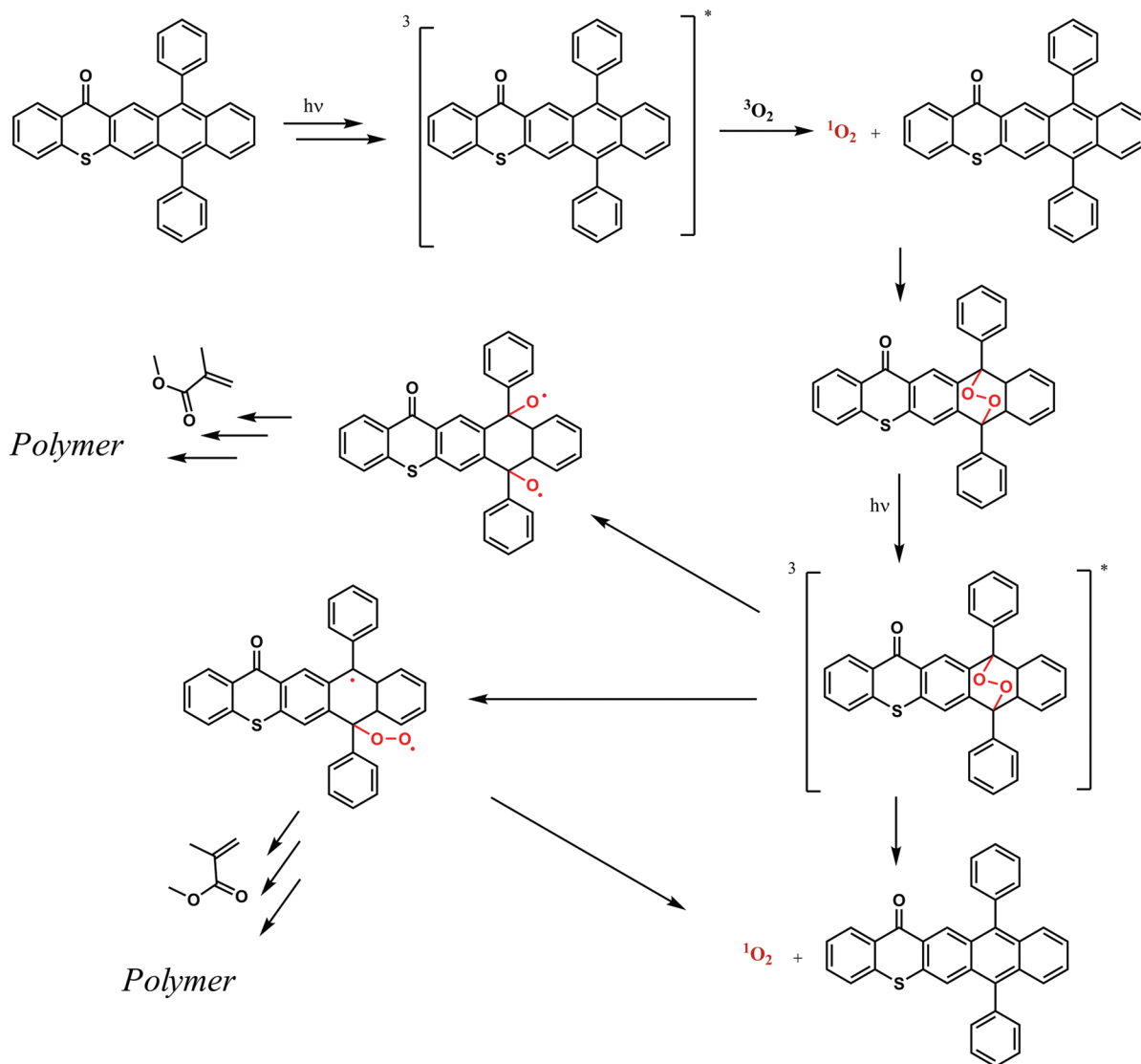
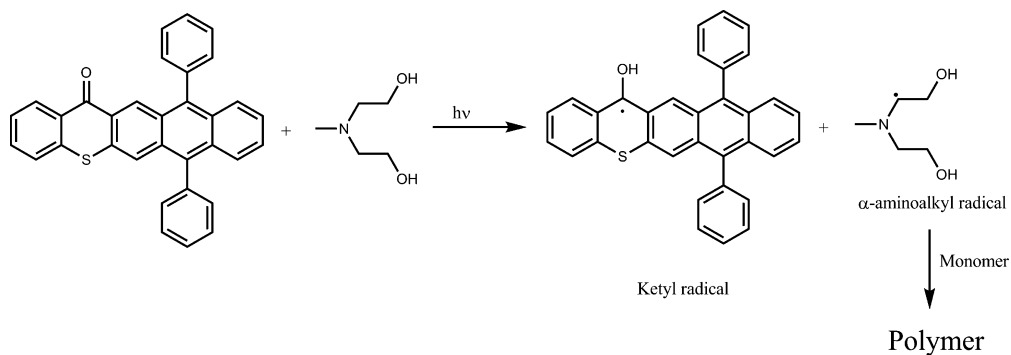
In conclusion, diphenylanthracene (TX-DPA) was successfully synthesized and was found to have excellent optical properties in the visible region of the electromagnetic spectrum. TX-DPA initiated polymerization of methyl methacrylate in the presence and absence of oxygen. The initiation mechanism in the presence of oxygen possibly explains the involvement of the formation of singlet oxygen by energy transfer from triplet TX-DPA and resulted in alkoxy or peroxy radicals after photo-excitation of TX-DPA- O_2 initiated free radical polymerization. High molar absorptivity in the visible region may possibly lead to using this photoinitiator in long wavelength region applications in the presence of oxygen atmosphere.

EXPERIMENTAL SECTION

Materials. 9,10-Diphenylanthracene (DPA, 97%, Aldrich) thio-salicylic acid (98.5%, Fluka), glacial acetic acid (Aldrich), N-methyldiethanolamine (MDEA, 99%, Aldrich), sulfuric acid (H_2SO_4 , 98%, Merck), ethanol (HPLC grade, Aldrich), acetonitrile (HPLC grade, Aldrich), chloroform (CHCl_3 , $\geq 99.8\%$, Fluka), N,N'-dimethyl-formamide (DMF, $\geq 99\%$, Aldrich) and thioxanthone (TX, $\geq 98.5\%$, Fluka) were used as received. Methyl methacrylate (MMA, $\geq 99\%$, Fluka) was washed with 5% aqueous NaOH solution, dried over CaCl_2 , and distilled over CaH_2 in vacuo. Tetrahydrofuran (99.8%, J.T. Baker) was dried and distilled over LiAlH_4 .

Synthesis of 7,12-Diphenyl-14H-naphtho[2,3-b]thioxanthene-14-one (TX-DPA). A heated solution of 9,10-diphenylanthracene ($2 \times 10^{-3} \text{ mol}$) in glacial acetic acid (15 mL) was added slowly to the thio-salicylic acid ($2 \times 10^{-3} \text{ mol}$) under stirring followed by the addition of 5 mL concentrated sulphuric acid. After the addition, the reaction mixture was refluxed at 120°C for 5 h after which it was left to stand at room temperature overnight. The resulting mixture was poured carefully under stirring into a 10-fold excess of boiling water. The mixture was stirred under boiling for an additional 5 min. The

Scheme 3. Photoinduced Radical Generation Mechanism of TX-DPA Photoinitiator in the Presence of Oxygen

Scheme 4. Photoinduced radical generation mechanism of TX-DPA photoinitiator with *N*-methyl-diethanolamine

solution was cooled and filtered. The residue product was purified by column chromatography over silica gel eluting with chloroform (Chart 2). M_A ($\text{C}_{33}\text{H}_{20}\text{OS}$): 464 g mol⁻¹; yield: 52%; mp 263–266 °C.

¹H NMR (500 MHz) in CDCl_3 : δ 8.03 (d, J = 8.78 Hz, 1H, H_{13}), 7.62 (d, J = 8.78 Hz, 1H, H_6), 7.61 (dd, J = 8.78 ; Hz, 1H, H_3), 7.55–7.48 (m, 4H, H_1 , H_2 , H_8 , H_{11}), 7.42–7.38 (m, 5H, H_{15} , H_{15} , H_{16} , H_{16} , H_{17}), 7.38–7.28 (m, 4H, H_{18} , H_{18} , H_{19} , H_{19}), 7.21–7.15 (m, 3H, H_9 , H_{10} , H_{20}), 7.08 (d, J = 8.78 Hz, 1H, H_4) ppm.

IR(KBr): ν (cm⁻¹) aromatic (C–H: 3053), ketone (C=O: 1634), (C=C: 1590).

Anal. Calcd for $\text{C}_{33}\text{H}_{20}\text{OS}$ (464.12 g mol⁻¹): C, 85.31; H, 4.34; S, 6.90. Found, C, 85.29; H, 4.35; S, 6.90.

Photopolymerization. Appropriate solutions of the monomer and TX-DPA in DMF in the absence and presence of *N*-methyl-diethanolamine (MDEA) were irradiated in a photoreactor consisting of a 400 W medium pressure mercury lamp with a water cooling system and simultaneously irradiated in a photoreactor

consisting of a 400 W xenon lamp with a water cooling system, in an air atmosphere. Polymers were obtained after precipitation in methanol and drying *in vacuo*. Conversions were calculated for all samples gravimetrically.

Analyses. GPC analyses of the polymer were performed at room temperature with a setup consisting of a pump (Agilent 1100) and three columns (Zorbax PSM); THF was used as the eluent (flow rate 0.3 mL min⁻¹), and detection was carried out with the aid of an Agilent 1100s differential refractometer. The number-average molecular weights were determined using Polymer Laboratories polystyrene standards. UV-vis spectra were taken on an Agilent 8453. IR spectra were recorded on an ATI Unicam Mattson 1000 FT/IR-3 spectrophotometer on a KBr disk. Fluorescence spectra were recorded on a Jobin Yvon-Horiba Fluoromax-P.

AUTHOR INFORMATION

Corresponding Author

*Telephone: + 90 212 383 4186. Fax: +90 212 383 4134. E-mail: narsu@yildiz.edu.tr.

REFERENCES

- (1) Fouassier, J. P. *Photoinitiation, Photopolymerization and Photocuring, Fundamentals and Applications*; Hanser Verlag: Munich, Germany, 1995.
- (2) Dietliker, K. *Chemistry & Technology of UV & EB Formulation for Coatings, Inks & Paints*; SITA Technology Ltd.: London, 1991.
- (3) Davidson, R. S. *Exploring the Science, Technology and Applications of UV and EB Curing*; SITA Technology Ltd.: London, 1999.
- (4) Dietliker, K. In *Chemistry & Technology of UV & EB Formulation for Coatings, Inks & Paints*, 2nd ed.; SITA Technology Ltd.: London, 1998; Vol. 3.
- (5) Hageman, H. S. *Photopolymerization and Photoimaging Science and Technology*; Elsevier: London, 1989.
- (6) Wayne, R. P. *Photochemistry*; University Lectures: London, 1970.
- (7) Mishra, M. K.; Yagci, Y. *Handbook of Radical Vinyl Polymerization*; Marcel Dekker Inc.: New York: 1998; Chapter 7.
- (8) Davidson, R. S. In *Advances in Physical Chemistry*; Bethel, D., Gold, V., Eds.; Academic Press: London, 1983; p 1.
- (9) Encinas, M. V.; Rufs, A. M.; Corrales, T.; Catalina, F.; Peinado, C.; Schmith, K.; Neumann, M. G.; Allen, N. S. *Polymer* **2002**, *43*, 3909–3913.
- (10) Corrales, T.; Catalina, F.; Peinado, C.; Allen, N. S.; Rufs, A. M.; Bueno, C.; Encinas, M. V. *Polymer* **2002**, *43*, 4591–4597.
- (11) Corrales, T.; Catalina, F.; Allen, N. S.; Peinado, C. *J. Photochem. Photobiol. A: Chem* **2004**, *169*, 95–100.
- (12) Vazquez, B.; Levenfeld, B.; Roman, J. S. *Polym. Int.* **1998**, *46*, 241–250.
- (13) Paul, S.; *Surface Coating: Science & Technology*; Wiley-Interscience: New York, 1986.
- (14) Jiang, X.; Xu, H.; Yin, J. *Polymer* **2004**, *45*, 133–140.
- (15) Jiang, X.; Yin, J. *Polymer* **2004**, *45*, 5057–5063.
- (16) Pouliquen, L.; Coqueret, X.; Moret-Savary, F.; Fouassier, J. P. *Macromolecules* **1995**, *28*, 8028–8034.
- (17) Wen, Y. N.; Jiang, X. S.; Yin, J. *Polym. Eng. Sci.* **2009**, *49*, 1608–1615.
- (18) Wen, Y. N.; Jiang, X. S.; Yin, J. *Prog. Org. Coat.* **2009**, *66*, 65–72.
- (19) Wei, J.; Liu, F. *Macromolecules* **2009**, *42*, 5486–5491.
- (20) Temel, G.; Aydogan, B.; Arsu, N.; Yagci, Y. *Macromolecules* **2009**, *42*, 6098–6106.
- (21) Allen, N. S.; Lam, E.; Kotecha, J. L.; Green, W. A.; Timms, A.; Navaratnam, S.; Parsons, B. J. *J. Photochem. Photobiol. A: Chem.* **1990**, *54*, 367–388.
- (22) Allen, N. S.; Lam, E.; Howells, E. M.; Green, P. N.; Green, A.; Catalina, F.; Peinado, C. *Eur. Polym. J.* **1990**, *26*, 1345–1353.
- (23) Aydin, M.; Arsu, N.; Yagci, Y. *Macromol. Rapid Commun.* **2003**, *24*, 718–723.
- (24) Aydin, M.; Arsu, N.; Yagci, Y.; Jockusch, S.; Turro, N. J. *Macromolecules* **2005**, *38*, 4133–4138.
- (25) Balta, D. K.; Temel, G.; Aydin, M.; Arsu, N. *Eur. Polym. J.* **2010**, *46*, 1374–1379.
- (26) Karaca, N.; Temel, G.; Balta, D. K.; Aydin, M.; Arsu, N. *J. Photochem. Photobiol. A: Chem.* **2010**, *209*, 1–6.
- (27) Yilmaz, G.; Aydogan, B.; Temel, G.; Arsu, N.; Moszner, N.; Yagci, Y. *Macromolecules* **2010**, *43*, 4520–4526.
- (28) Cokbaglan, L.; Arsu, N.; Yagci, Y.; Jockusch, S.; Turro, N. J. *Macromolecules* **2003**, *36*, 2649–2653.
- (29) Temel, G.; Arsu, N. *J. Photochem. Photobiol. A: Chem.* **2009**, *202*, 63–66.
- (30) Temel, G.; Karaca, N.; Arsu, N. *Polym. Sci., Polym. Chem. Ed.* **2010**, *48* (23), 5306–5312.
- (31) Carlini, C.; Angiolini, L.; Caretti, D.; Corelli, E. *Polym. Adv. Tech.* **1996**, *7*, 379–384.
- (32) Jiang, X. S.; Luo, J.; Yin, J. *Polymer* **2009**, *50*, 37–41.
- (33) Jiang, X. S.; Luo, X. W.; Yin, J. *J. Photochem. Photobiol. A: Chem.* **2005**, *174*, 165–170.
- (34) Balta, D. K.; Cetiner, N.; Temel, G.; Turgut, Z.; Arsu, N. *J. Photochem. Photobiol. A: Chem.* **2008**, *199*, 316–321.
- (35) Temel, G.; Arsu, N. *J. Photochem. Photobiol. A: Chem.* **2007**, *191* (2–3), 149–152.
- (36) Balta, D. K.; Arsu, N.; Yagci, Y.; Jockusch, S.; Turro, N. J. *Macromolecules* **2007**, *40*, 4138–4141.
- (37) Gacal, B.; Akat, H.; Balta, D. K.; Arsu, N.; Yagci, Y. *Macromolecules* **2008**, *41*, 2401–2405.
- (38) Akat, H.; Gacal, B.; Balta, D. K.; Arsu, N.; Yagci, Y. *J. Polym. Sci., Polym. Chem. Ed.* **2010**, *48*, 2109–2114.
- (39) Balta, D. K.; Arsu, N.; Yagci, Y.; Sundaresan, A. K.; Jockusch, S.; Turro, N. J. *Macromolecules* **2011**, *44* (8), 2531–2535.
- (40) Balta, D. K.; Arsu, N. *J. Photochem. Photobiol. A: Chem.* **2008**, *200*, 377–380.
- (41) Morris, J. V.; Mahaney, M. A.; Huber, J. R. *J. Phys. Chem.* **1976**, *80*, 969–974.
- (42) Dalton, J. C.; Montgomery, F. C. *J. Am. Chem. Soc.* **1974**, *96*, 6230–6232.
- (43) Amirzadeh, G.; Schnabel, W. *Macromol. Chem.* **1981**, *182*, 2821–2835.
- (44) Stevens, B.; Small, R. D. Jr. *J. Am. Chem. Soc.* **1977**, *81*, 1605–1606.
- (45) Monroe, B. M. *J. Phys. Chem.* **1978**, *82*, 15–18.
- (46) Olea, A. F.; Wilkinson, F. *J. Phys. Chem.* **1995**, *99*, 4518–4524.
- (47) Schmidt, R.; Brauer, H. D. *J. Photochem.* **1986**, *34*, 1–12.
- (48) Wilson, T.; Catalani, L. H. *J. Am. Chem. Soc.* **1989**, *111*, 2633–2639.
- (49) Jesse, K.; Comes, F. J. *J. Phys. Chem.* **1991**, *95*, 1311–1315.